Droplet Formation and Growth in Polluted Fogs

Frank, Göran; Martinsson, Bengt; Cederfelt, Sven-Inge; Berg, Olle; Swietlicki, Erik; Wendish, Manfred; Yuskiewicz, Brett; Heintzenberg, Jost; Wiedensohler, Alfred; Orsini, Douglas; Stratmann, Frank; Laj, Paolo; Ricci, Loretta

Published in:
Contributions to Atmospheric Physics

1998

Contr. Atmos. Phys., February 1998, p. 65–85
0005-8173/98/01 0065-21 $ 3.00/0

Droplet Formation and Growth in Polluted Fogs

GÖRAN FRANK[1], BENGT G. MARTINSSON [1], SVEN-INGE CEDERFELT[1], OLLE H. BERG[1], ERIK SWIETLICKI[1], MANFRED WENDISCH[2], BRETT YUSKIEWICZ [2], JOST HEINTZENBERG[2], ALFRED WIEDENSOHLER[2], DOUGLAS ORSINI[2], FRANK STRATMANN[2], PAOLO LAJ[3], AND LORETTA RICCI[3]

[1] Div. of Nuclear Physics, Lund Institute of Technology, Lund University, P.O. Box 118, S 221 00 Lund, Sweden
[2] Institute for Tropospheric Research, Permoserstr. 15, D 04303 Leipzig, Germany
[3] Istituto FISBAT - CNR, Via Gobetti 101, I 40129 Bologna, Italy

(Manuscript received February 04, 1997; accepted December 15, 1997)

Abstract

Fog droplet formation and growth related to fog droplet activation were studied in a polluted region. The joint field experiments were carried out at San Pietro Capofiume in northern Italy during November 1994. It was found that the fog droplet number distribution was continuous in the size region 1–47 μm and that for most of the time the fog consisted of unactivated droplets, i.e. the droplets were smaller than the critical diameter for activation according to the Köhler equation. During a few time periods some of the droplets were possibly slightly larger than the critical diameter for activation. The solute concentration in the fog droplets was found to be strongly dependent and decreasing with increasing droplet size. The experimental results were compared with results obtained using a fog model. Good overall agreement was found between the model and the experimental results, with respect to fog droplet size related to dry residue size, and to fog droplet number distribution. The fog model was also used to study the influence on fog droplet growth of the rate of temperature decrease, the aerosol particle mass load and fog liquid water content. In addition the effect of aging of the fog was also considered.

1 Introduction

The physical and chemical interactions between gases, aerosol particles and liquid water droplets in fogs and clouds can influence the composition of the troposphere, the chemical composition of the gas phase and also that of the particulate matter, as well as modify the physical properties of the particles. This will affect transport and deposition of pollutants, visibility, radiative properties, climate, etc. Studies of these processes are therefore essential to understand the role of fogs and clouds in the atmosphere.

Fog and cloud droplets are formed by condensation of water vapour onto the aerosol particles present at an elevated relative humidity in the atmosphere. The formation of droplets can begin during sub saturated conditions because ionic species such as ammonium, nitrate and sulphate are soluble, i.e. particles containing ionic species takes up water vapour and form highly concentrated liquid particles. The droplet (or liquid particle) adopts a relative humidity dependent equilibrium size in relation to the water vapour equilibrium conditions.

At a slight supersaturation, when the relative humidity can become greater than the critical value, the droplet will leave the equilibrium state and grow without limitation (except dynamic) by condensation of water vapour. This is called activation and the droplet diameter of activation is called the critical diameter for activation.

Growth and activation of fog and cloud droplets are described by the Köhler equation, which describes the equilibrium state and the critical diameter for activation of an individual droplet (Pruppacher and Klett, 1980). The equilibrium condition is controlled

by condensation and evaporation of water vapour and is described by a combination of the curvature effect of the droplets (Kelvin effect) and the water activity, i.e. the presence of water soluble material which in idealised form is described by Raoult's law.

Droplet growth at low relative humidities cannot be properly described by Raoult's law. Chen (1994) presented a modified Köhler equation which consider deliquescence and also hysteresis processes of pure salts. At supersaturated conditions the situation may also be somewhat further complicated by the presence of surface active and water soluble organic compounds (Gill et al., 1983; Saxena et al., 1995; Laaksonen et al., 1997). The effect of the organic compounds cannot as yet be quantitatively related to known atmospheric conditions.

The critical relative humidity and hence the critical droplet diameter are specific for each droplet and depend on the size and chemical composition of the original dry particle (Hänel, 1976; Martinsson et al., 1997; Svenningsson et al., 1997). Thus, the more ions that are available in the dissolved particle, the lower is the degree of supersaturation required with respect to water vapour, which implies that large particles with a large fraction of water soluble material are more easily activated.

The largest droplets can however have difficulties in following the equilibrium conditions after a change in ambient relative humidity due to mass transport limitations (Hänel, 1987; Pandis et al., 1990). The first activated particles will therefore be the medium size particles (as dry diameter) followed by the smaller and larger particles. Thus after activation there will be the following three types of particles and droplets in a cloud or fog: 1. Small non-activated particles at equilibrium conditions, called the interstitial aerosol particles, 2. Activated droplets, 3. Large non-activated droplets. The group of large non-activated droplets can in certain circumstances, although they are not activated, carry a significant amount of liquid water.

The present study was undertaken in a fog which formed within a polluted aerosol. Such a system has been investigated in an earlier study, using a counterflow virtual impactor (CVI) system, with respect to both droplet nucleation scavenging and size dependent droplet solute concentration. In that study the scavenging was defined according to a fixed ambient (droplet) diameter (Noone et al., 1992). The solute concentration of the fog droplets was found to decrease with droplet size (Ogren et al., 1992).

The objectives of this study are to characterise the fog microstructure in more detail, with respect to:

(a) fog droplet size distribution

(b) fog droplet diameter related to activation (critical diameter)

(c) the size-dependent fog droplet solute concentration

It was found that most of the time the fog consisted of unactivated droplets, which explained the microstructure characterised by a continuous droplet size distribution (no gap between activated and unactivated droplets) with a small mode of large droplets nucleated on the largest particles. This also explained the decreasing fog droplet solute concentration with increasing fog droplet diameter. The intrinsic features of droplet growth in a reservoir of droplets was studied in relation to these results using the fog model. This was used to investigate the influence on the fog microphysics of various parameters such as: aerosol particle mass load, the dynamics in association with the onset and development of the fog and aging of the fog.

The results presented are, amongst other techniques, based on the use of the droplet aerosol analyser (DAA), where the ambient droplet size (activated or unactivated) is determined together with the size of its dry residue (the reminder of a diffusion dried droplet or particle). This instrument also measures the number concentration which provides a third variable to the data set as follows: ambient size, dry residue size and number concentration. Having access to these droplet parameters and also the hygroscopic properties, a number of related aerosol/cloud variables, such as solute concentration, ambient and dry residue size distributions and the activation status of a droplet, can be determined. As a consequence the fog can be characterised in relation to the droplet activation as defined by the Köhler equation.

2 Experimental And Modelling Methods

The experiments were undertaken in November 1994, outside San Pietro Capofiume located in the Po Valley in northern Italy, as part of a joint field study (CHEMDROP – Chemical composition and processes in clouds and fogs: Dependence on the size of particles and droplets) involving six institutions. An overview of the CHEMDROP-experiment, including meteorology during the campaign, is presented by Fuzzi et al. (1998). A description of the measuring site can be found in Fuzzi et al. (1992). This paper will primarily deal with the fog / aerosol interface, the size dependence of the droplet solute

concentration and the microphysical structure of the fog, as related to droplet activation, primarily based on the experimental data obtained by the DAA. The data will be presented together with the results from fog modelling.

2.1 The Droplet Aerosol Analyser (DAA)

The DAA was in operation approximately 300 hours during fog, mist and haze conditions. A description together with theoretical background of the instrument can be found in Martinsson (1996). A detailed description of the instrument and a field intercomparison with the particulate volume monitor (PVM), differential mobility particle sizer (DMPS) and the forward scattering spectrometer probe (FSSP), with respect to six aerosol and cloud characteristics can be found in Cederfelt et al. (1997).

The instrument makes use of aerosol charging mechanisms, diffusion drying of droplets and also electrostatic aerosol spectrometry, in a multi-step processing system, to determine the ambient (droplet) size and the dry size. Together with particle counting this gives a three parameter data-set comprising of: ambient (droplet) diameter, dry diameter and number concentration.

The air inlet was placed 5 m above the ground. The DAA mode of operation is such that the ambient (droplet) diameters interrelated with twelve different dry residue diameters (three at a time) are determined. The residue diameters are set and the DAA scans over the droplet diameter. After a complete scan over the droplet sizes, the three residue diameters were changed to three new sizes, according to a computer-controlled repetitive schedule comprising of four different settings and thus twelve dry residue sizes. The twelve sizes were chosen from a relatively narrow size interval, in order to account for the fine structure, if present, of the droplet growth related to the dry residue size.

During the first fog event of this campaign it was found that significant amounts of water were associated with the large particles, therefore the dry sizes monitored were changed during the campaign. Up to midday of 15th November the dry diameters 0.21, 0.23, 0.26, 0.30, 0.34, 0.39, 0.44, 0.51, 0.58, 0.67, 0.78 and 0.9 μm were measured during the four scans, with each fourth size belonging to the same scan. After this date the smallest particle size was replaced by measurements at 1.05 μm, i.e. the measurement interval with respect to dry diameter was changed to 0.23 – 1.05 μm.

The three dry residue sizes measured during a scan were spaced by a factor of two with respect to electrical mobility. In order to account for the influence of particles larger than the sizes actually measured, the dry residue size distribution was extrapolated by a factor of two towards larger sizes with respect to electrical mobility. By this approach the associated droplet and residue sizes for three residue sizes were obtained in 15 min., the duration of one scan. Since four different settings of the residue sizes were used, the time between repeat measurements was one hour for a given residue size.

One scan of the DAA results in measurements of the charge distributions related to the dry residue sizes. The droplet sizes was determined from the charge distributions after calibration of the instrument. However, at present time this is incomplete. Calibration of the average charge as a function of droplet size have been made using monodisperse droplets of di-octyl phthalate in the range 0.1 to 10 μm in diameter (Cederfelt and Martinsson, 1996). The calibration with respect to the width of the charge distribution as a function of droplet size is in progress. As a consequence, no results on the width of the droplet distribution for a specific residue size can be given at this stage. Thus, the data will be presented in the form of average ambient diameter.

The droplet number distribution resulting from nucleation on the dry residue size region studied (i.e. the upper accumulation mode particles), was obtained by fitting a function to the relationship between droplet diameter and the dry residue diameter. The function was differentiated, and the droplet size distribution was obtained from:

$$\frac{dN}{d\log D_d} = \frac{dN}{d\log D_p}\frac{d\log D_p}{d\log D_d} \qquad (2.1)$$

where N is the number concentration, D_d the ambient diameter and D_p the dry residue diameter.

During the campaign the DAA unipolar charging unit suffered from a malfunction, which resulted in too low charge levels on the droplets. The problem was caused by leakage around a net used to smooth the flow profile of the charging unit. This may alter the flow profile and hence the time available for the charging process. In order to overcome the problem, the DAA results were compared with the hygroscopic growth factors determined using the TDMA, for cases where the ambient relative humidity was close to the humidity used in the TDMA (i.e. 90% relative humidity). Thus, for all cases where both the DAA and the TDMA were in operation and the ambient relative humidity was close to 90%, the ambient

size determined by the DAA for a given residue size, were compared with the size obtained by multiplying the dry size by the growth factor from the TDMA for the same residue size. It was found that the size determined using the DAA was 30% lower. In order to correct the DAA data set, the charging time in the unipolar charging unit was therefore changed accordingly. Thus the non-dimensional charging time (Klett, 1971) was found to be 0.18, normally the value is 0.26 in the DAA charger.

The errors in determining the ambient (droplet) diameter can be derived from three uncertainties:

(a) Imprecision due to malfunction of the charger, resulting in a relative standard deviation in droplet diameter of 10%.

(b) Imprecision due to low counting statistics, which was negligible except for the largest dry residue sizes measured. For these the relative standard deviation in ambient diameter was 10%.

(c) Inaccuracy in the calibration of the unipolar charger, resulting in a relative standard deviation of 10% for droplets larger than 0.1 μm in ambient diameter.

Thus, the typical relative error (one relative standard deviation) in ambient (droplet) diameter was 15% for droplets related to dry residue diameters smaller than 0.8 μm and 17% for droplets related to dry residue diameters larger than 0.8 μm.

2.2 Complementary Techniques

In order to describe the microstructure of the fog, data from other types of instruments are required.

Data from a tandem differential mobility analyser (TDMA) was used to obtain the size-dependent hygroscopic properties of the particles. The TDMA relates the particle diameter at 90% relative humidity (RH) to the diameter at less than 20% RH. The hygroscopic growth of a single particle size could sometimes be represented by one mode, especially for large particles. Most commonly it was bimodal and occasionally tri-modal. The TDMA is described, together with results from this campaign by Berg et al. (1998). The average hygroscopic growth was used as the basis of estimating the composition of the particles, assuming that each particle consists of salt and hygroscopically inactive material (Svenningsson et al., 1994). The results obtained during these experiments showed a good agreement between TDMA and the chemical analyses of the size resolved aerosol impactor measurements (Ricci et al., 1998). It was found that ammonium, nitrate and sulphate were the dominating ionic species. In diluted solutions of these species, the hygroscopic growth is similar to that of ammonium sulphate, which was used as the model substance and in the calculations of the solute concentrations.

A forward scattering spectrometer probe (FSSP) (Knollenberg, 1981) was used to measure the ambient (droplet) size number distribution in the size region 2 to 47 μm in diameter, with the size resolution 3 μm. The channel size of the smallest droplets (2–5 μm) was considered unreliable (Wendisch et al., 1998) and was therefore not used. The integral of the FSSP volume distribution was used as the measure of fog liquid water content (LWC). The instrument is described in more detail, together with results from this campaign in Wendisch et al. (1998).

Size resolved fog droplet impactor sampling and chemical analyses were used to determine ionic composition of the fog droplets, which in this paper we have used to compare size dependent solute concentrations and also to estimate the size dependent number of ions of soluble species per droplet. The sizes measured were: 7.5, 12.5, 17.5, 21.5, 27.5 and 39.5 μm ambient diameter (mid-diameter of the impactor steps). The impactors and chemical analyses are described in more detail by Laj et al. (1998).

The sub-micrometre dry aerosol particle distributions from 0.003 to 0.85 μm dry diameter were determined using a differential mobility particle sizer (DMPS). The instrument and data from this campaign are described by Yuskiewicz et al. (1998). Data from a DMPS with the inlet at a height of 5 m, was used as input data for the model studies. The inlet had an impactor cut-off of 5 μm ambient diameter, which removed droplets larger than this size from the aerosol being sampled.

The atmospheric visibility measured during this campaign (Heintzenberg et al., 1998) was used to classify the DAA-data. The LWC measured using a particulate volume monitor (PVM) (Wendisch et al., 1998) was used for the selection of the cases studied, to obtain as constant LWC as possible during the periods selected.

The ambient relative humidity was measured using a Philips 2322 humidity sensor and an electric ventilated psychrometer.

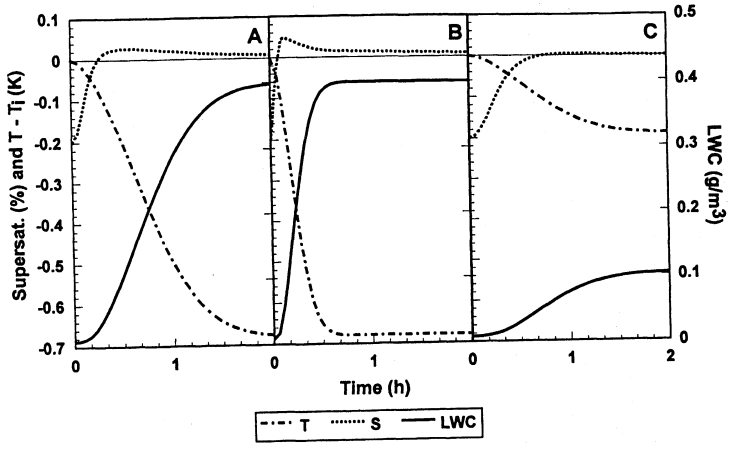

Figure 1: Three examples of temperature evolution used to produce the fog, as a function of time. The resulting supersaturation ($100(s-1)$, s = water vapour saturation ratio) and fog LWC, as a function of time are also shown. (a) $c = 1 \times 10^{-7}$ s^{-2} and $(T_i - T_f) = 0.67$ K, (b) $c = 1 \times 10^{-6}$ s^{-2} and $(T_i - T_f) = 0.67$ K, (c) $c = 1 \times 10^{-7}$ s^{-2} and $(T_i - T_f) = 0.18$ K.

2.3 Modelling Techniques

A model of fog droplet formation and growth was used as the means of relating the experimental observations with theory. It treats the humid air as a closed air parcel, i.e. all parts of the air mass experience the same relative humidity history. In this model, which is of the particle-tracing type (Young, 1993), the aerosol particle size distribution is described by 70 size groups per decade in the dry particle size interval 0.05–15 μm, in a total 173 particle size groups. The expressions for the droplet growth rate and the modified form of the vapour diffusivity and the thermal conductivity are based on the formulations by Pruppacher and Klett (1980).

This model has been applied to a study of orographic clouds by Martinsson et al. (1997) where the adiabatic cooling of the air parcel was driven by the updraught velocity of the air mass. In the present fog study, the air mass was cooled by an isobaric process. The fog was produced using an initial saturation ratio of 0.998, by applying the following expression for the air mass temperature (T):

$$\frac{dT}{dt} = 2cte^{-ct^2}\left(T_f - T_i - \frac{w_{Lf}L_e}{C_{pa}(1-e^{ct_f^2})}\right) + \frac{dw_L}{dt}\frac{L_e}{C_{pa}} \qquad (2.2)$$

where t is the time, w_L is the LWC, L_e the latent heat of evaporation and C_{pa} the heat capacity of air. The initial and final temperatures of the fog (T_i and T_f), the final LWC of the fog (w_{Lf}), the duration of the model (t_f) together with the constant c, which was used to vary the rate of temperature decrease, were given as input parameters. This expression produces a temperature variation of basically the form $(T_f - T_i)(1 - \exp(-ct^2))$, with some disturbance of the overall curve due to the latent heat of the condensation. Thus, the temperature decreases from the initial value, at a rate determined by the constant c and after sufficient time the temperature remains constant at its final value.

The water vapour saturation ratio change was computed in the model from the relations in the water vapour mixing ratio, the temperature and the air expansion (the latter was negligible in this study). Three examples of the development of the fog, with all model input parameters the same except for the value of the constant c and $(T_i - T_f)$ (and hence the final LWC produced) of the air mass are shown in Figure 1. This shows how the temperature profiles change with the value of the constant c and, as a consequence, the time required to produce the final value of the LWC. This also leads to the case where a rapid temperature decrease occurs, which produces an earlier supersaturation and also a higher peak supersatu-

ration. It can also be seen that a reduced value in the LWC, results in the air mass barely reaching supersaturation.

The dry particle size distribution used as the input in the sub-micrometer region was based on measurements by the DAA and a DMPS. The dry size distribution of the super-micron particles was not determined. The input to the model in this region was based on estimates from the FSSP and the size-resolved fog impactor, together with DAA data. The basis of this estimation is presented in Section 3.2. Organic substances may influence the interaction between aerosol particles and water during fog formation, by entering the solution at a high relative humidity (Shulman et al., 1996), compared to the conditions in measurements by the TDMA at 90% relative humidity. They may also affect the surface tension of the fog droplets (Capel et al., 1990). It is, however, beyond the scope of this paper to investigate these effects in the modelling because no experimental data on the organic constituents are available for comparison from this campaign. The effects of organic compounds are discussed further in Section 3.4. In the model the droplets were treated as ionic solutions, containing an insoluble fraction of particulate matter, which was deduced from the TDMA measurements (see Section 2.2), with the water activity described by Raoult's law (in Raoult's law the number of moles of ions of the soluble substances was used).

3 Results

3.1 Fog Definition

During the experimental period there were nine fog events (Fuzzi et al., 1998) and the DAA was operating during events one to three and from five to seven. During the remaining time of the field campaign, the visibility was never more than 2500 m, which means that we experienced misty or hazy conditions during that time. The DAA was in operation approximately 300 hours during the campaign including 40 hours of fog.

Table 1: Definition of fog, mist and haze according to atmospheric visibility.

Visibility	Weather Condition
< 500 m	Fog
500 – 1000 m	Mist
> 1000 m	Haze

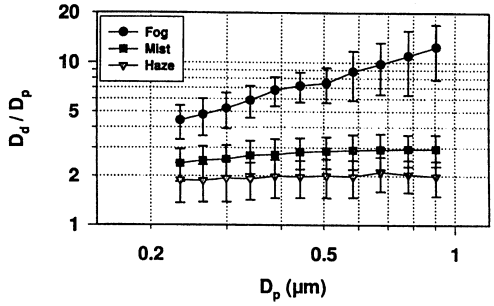

Figure 2: Average growth factor (D_d/D_p) over the campaign for the three weather conditions: fog, mist and haze, as function of dry residue diameter. The bars show the standard deviation (±) from the mean. D_d = ambient (droplet) diameter. D_p = dry residue particle diameter.

The DAA data has been grouped into the three weather conditions namely: fog, mist and haze according to visibility measurements, see Table 1. The characteristics of these are given by Heintzenberg et al. (1998). The growth factor (ambient diameter / dry diameter) connected with the dry residue diameters measured by the DAA (0.2 – 0.9 µm) for the above conditions are shown in Figure 2, for each of the eleven residue sizes measured during the whole campaign. The data are mean values for the whole campaign for the respective condition. The average droplet growth factors during the haze were about 2 and almost constant for all the dry diameters measured. Haze is associated with the lowest relative humidity (RH). At higher RH, during misty periods, the growth factors show a slight size dependency. A small increase from 2.5 to 3 was observed with increasing dry diameter. During fog periods (RH close to 100%) the growth factors are drastically different. The growth factors for the fog are significantly larger than for mist and haze, which of course is expected, they are also strongly dependent on particle diameter. This can be explained by the Köhler equation which shows that, when close to saturation, a small change in RH will produce a larger change in ambient droplet size for the larger droplets. This means that the largest droplets will vary their size more with changing RH, than smaller droplets. This explanation is valid if the droplets are unactivated and in equilibrium conditions, since activated droplets do not assume an equilibrium size.

This paper primarily deals with the fog microstructure. The data from all fog events during the campaign are shown in Figure 3, as ambient size related

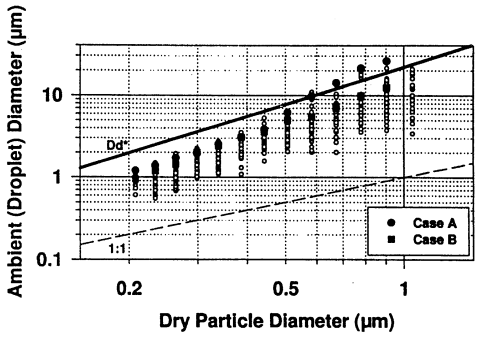

Figure 3: Fog data measured by DAA during the campaign. The results are presented as ambient (droplet) diameter as function of dry residue diameter. Every point represents a 15 minute sample. The bold line shows the critical diameter according to the Köhler equation for particles consisting of 50% unsoluble matter and 50% ammonium sulphate. Case A and case B were chosen for more detailed studies. Note that the smallest (0.21 µm) and the largest (1.05 µm) dry residue sizes were not measured during the whole campaign.

Table 2: Two cases selected for further studies.

Case	Time period	LWC (mg m^{-3}) (measured with FSSP)
A	November 13, 22:20-23:20	460
B	November 15, 07:15-08:15	380

to the dry residue size. The critical diameter for activation for a particle consisting of 50% insoluble material and 50% ammonium sulphate is shown in Figure 3. This shows the approximate position of the critical diameter, which will be elaborated on in Section 3.4. It can be seen that most of the measurements fall well below the critical diameter. Droplets which are smaller than this critical diameter are unactivated.

Out of all the fog data, two one-hour cases were selected for more detailed study, see Table 2. In case A, during the first fog event, it can be seen that the larger droplets were slightly larger than the critical diameter indicated in Figure 3. This was chosen as the case which possibly represents droplet activation. Case B, during the second fog event, was chosen to be the example more representative of the usual situation found during the campaign.

3.2 Dry Particle Size Distribution

During the field campaign, the sub-micron particle size distribution (from 0.003 to 0.85 µm) was measured using a differential mobility particle sizer (DMPS). The DAA measured the dry particle size distribution from 0.2 to 1 µm, but unfortunately no size distribution measurements where made for super-micron particles (particles larger than 1 µm in diameter). As will be shown below, the super-micron particles are important in the fog formation. An estimation of their number and sizes was therefore made.

The FSSP measured the liquid water content (LWC) related to droplets with ambient diameter from 2 to 47 µm and this was used as the total LWC (Wendisch et al., 1998). The DAA measured the LWC associated with particles with dry residue diameters from 0.2 to 1 µm. The mass of water nucleated on particles smaller than 0.2 µm is unlikely to be large. The mean value of the LWC during case A, measured using a FSSP was 460 mg m^{-3} and by DAA, 70 mg m^{-3}. This indicates that most of the liquid water was associated with particles with a dry diameter of more than 1 µm during the fog. Figure 4 shows the normalized dry residue size dependent volume distribution, as measured by DAA, for the average dry particle distribution over the campaign and the average ambient volume distributions for the three defined weather conditions fog, mist and haze. The dry, haze and mist distributions show a similar appearance, which is to be expected from Figure 2, where it can be seen that

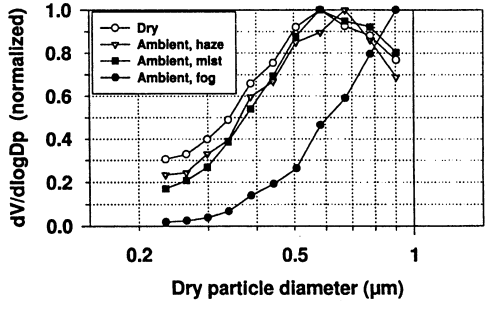

Figure 4: Normalized volume distribution of dry particles and ambient droplets of fog, mist and haze; measured by the DAA. The dry residue particles are presented as average volume distribution over the whole campaign and the fog; mist and haze distributions are based on the average ambient droplet volume during the respective weather conditions. All volume distributions are given as a function of dry residue diameter and are normalized individually to the maximum value of each of the distributions. The maximum in the volume distribution are at 0.6–0.7 µm in dry diameter for the dry, haze and mist distributions whereas the maximum of the fog distribution are at a higher dry diameter than 0.9 µm.

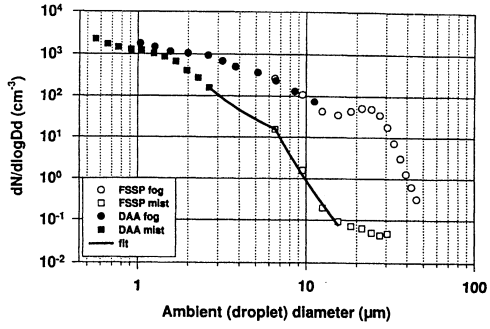

Figure 5: Average droplet number distributions for fog and mist measured by DAA and FSSP; as function of ambient (droplet) diameter (The FSSP data are from Heintzenberg et al. (1998)). The line represents a fit of the data during mist.

Table 3: Ionic concentration of droplets at various impactor steps. Maximum ambient (droplet) diameters measured by the DAA were for cases A; 26 µm and B; 12.5 µm; which corresponds to 0.9 µm in dry residue diameter.

Fog droplet impactor step (mid diameter) (µm)	Average ionic concentration in the droplets
Case A	
27.5	14.2×10^{-15}
39.5	23.3×10^{-15}
Case B	
12.5	14.3×10^{-15}
21.5	43.9×10^{-15}
27.5	34.6×10^{-15}
39.5	64.0×10^{-15}

the growth factors are almost constant in the size range measured. For the fog, the growth factors are increasing with diameter. This results in a completely different shape of the ambient volume distribution, with the largest volume fraction associated with the largest particles measured. Hence, this also indicates that most of the ambient (droplet) volume in the fog, is associated with the super-micron particles and the need of an estimation of their number and sizes.

In order to make the estimation of the number of particles larger than 1 µm in diameter and if possible the number distribution, two methods have been used. The first makes use of the average droplet number distributions of mist and fog presented by Heintzenberg et al. (1998). These distributions are measured by FSSP and DAA and are mean values for the different conditions (mist and fog) over the whole campaign (see Figure 5). The DAA measures the ambient diameter related to dry residue diameters from 0.2 to 1 µm and therefore the number distribution for the fog are at larger ambient diameters than for the mist (the particles have grown more). The FSSP measured the number distribution from 2 to 47 µm in ambient diameter. For the fog the distributions from the two instruments overlap, they fit smoothly together and form a continuum. A summation of the FSSP distribution from the largest ambient diameter obtained using the DAA (11 µm) up to 47 µm can be used to estimate the mean value of the number of super micron particles, this results in an estimated value of 17 particles/cm^3.

A similar estimation can be made for the mist. During the mist the growth factors were much smaller and from Figure 2 it can be seen that it is about 3 in the size range 0.2 to 0.9 µm in diameter. The mist curve in Figure 5 can be seen as a shift to the right of the dry particle number distribution. This show more clearly that droplets larger than the largest ambient diameter measured with the DAA, have a dry diameter of more than 1 µm. An integration of the fit shown in Figure 5, from 2.85 µm and upwards gave 18 particles/cm^3 . This is very close to the value integrated from the fog conditions and provides a clear indication that this really is the average number of super micron particles during the campaign.

The second method was used to estimate the distribution of soluble matter in the super micro metre particles. The purpose of this is to provide the fog model with input data. The droplet growth is primarily determined by the amount of soluble matter. Hence, the unknown fraction of insoluble matter (e.g. crustal material) is of secondary importance in this context. The estimates have been carried out by calculating the average number of ions (of soluble matter) per droplet from the size resolved fog droplet impactors (Laj et al., 1998), the results of which are presented in Table 3. The maximum ambient (droplet) diameter measured using the DAA, which corresponds to a diameter of 0.9 µm as dry residue, was in case A 26 µm and in case B 12.5 µm. The nearest impactor step was in case A 27.5 µm and in case B 12.5 µm. The following larger impactor steps in each respective case had greater numbers of mole ions per droplet which shows that droplets with these diameters must have been nucleated on particles containing larger amounts of soluble material, than the particles with dry diameter of 0.9 µm. The dry particle diameter is proportional to the cube root of the number of ions per droplet, which implies that the super micron particles are not very much larger than 1 µm, i.e.

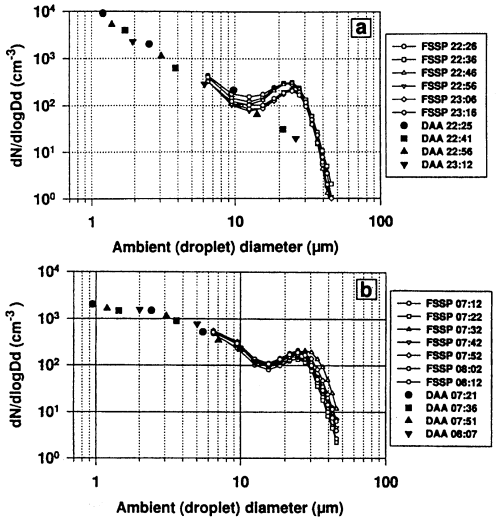

Figure 6: The number concentration of fog droplets as function of ambient (droplet) diameter. The numbers in the legend refer to the centre time of the sample averaging period. (a) Case A, (b) Case B.

they can be seen as a tail of the accumulation mode, at least with respect to the soluble matter.

3.3 Fog Droplet Size Distribution

This section presents the ambient (fog droplet) size distribution results based on the DAA and the FSSP data, in the two cases described in Section 3.1. The droplet number distributions determined using these techniques in cases A and B are shown in Figure 6. It should be kept in mind that the FSSP directly measures the ambient droplet size distribution from 2–47 μm (5 – 47 μm are used here) and that the DAA determines the size distribution of droplets related to particles with dry diameter of 0.2 – 0.9 μm, i.e. the upper part of the accumulation mode.

For case A, a fairly good agreement between the two instruments was found in the size region 5 – 15 μm, see Figure 6a. In the size range above 15 μm, the DAA results are significantly lower than those from FSSP. In Section 3.2 it was shown that a large amount of liquid water in fog was associated with particles with a dry diameter larger than the upper dry size limit of the DAA. The mode that can be observed by the FSSP, but not by the DAA, is therefore probably associated with these larger particles.

The results obtained in case B are shown in Figure 6b. From the DAA data it can be seen that the dry particle size region 0.2 – 0.9 μm is associated with the ambient diameter range 0.9 – 12 μm i.e. the growth is smaller than in case A. The size distributions obtained from the two instruments are in good agreement from 5 – 12 μm in ambient diameter and they therefore complement one other very well during this case. The only likely explanation for the droplets larger than 12 μm in diameter, which were observed by FSSP, is that they were formed on particles larger than the upper dry size limit of the DAA.

Hence, the DAA displays the droplet size distribution from the upper part of the accumulation mode, while the FSSP shows the droplet size distribution associated with particles with a dry diameter partly from the same size range as the DAA, but also from particles with dry diameter greater than 0.9 μm. The mode appearing around 25 μm in case A (Figure 6a), thus most probably consists of droplets nucleated on particles larger than approximately 0.8 μm, i.e. the upper tail of the accumulation mode and the coarse mode particles. The mode at 25 μm in case B (Figure 6b) most probably consist of droplets nucleated on particles larger than 1 μm in dry diameter.

On combining the information from both DAA and FSSP, it can be seen that the fog studied consisted of a continuous droplet number distribution on the time scales used (DAA $\approx$ 5 min, FSSP 1 min). No size region with a very low droplet number concentration which can be related to the droplet activation process (which was found in hill cap clouds (Martinsson et al., 1997)) was observed. The less pronounced modal structure observed, with the minimum around 15 μm diameter cannot, according to this analysis, be regarded as a limiting size with respect to droplet activation.

3.4 Fog Droplet Size Related to Activation

The fog droplet formation and growth have been analysed by relating droplet growth to activation, i.e. by directly relating the ambient diameter associated with the dry residue diameter, to the critical diameter for activation according to the Köhler equation. The relation between ambient and dry residue diameter for cases A and B is presented in Figure 7. The two cases are similar when the dry diameter is less than 0.5 μm, but for larger dry diameters case A displays considerably larger ambient diameters compared to case B. Case A was selected because it showed the strongest growth during the campaign, while case

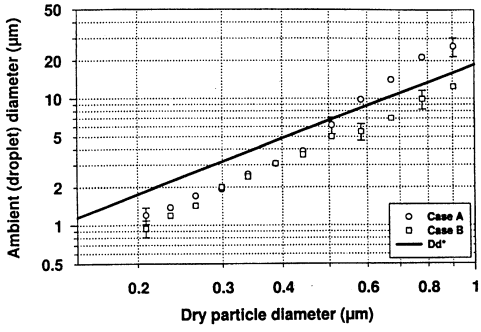

Figure 7: The ambient (droplet) diameter as function of dry residue diameter. The line represents the critical droplet diameter for activation; according to the Köhler equation based on hygroscopic growth measurements made by the tandem differential mobility analyser (TDMA). The bars show one standard deviation of the measurement error and the errors are in the same range for all presented droplet diameters; see Section 2.1.

B is representative of the usual situation during the campaign, see Figure 3. The bold line in Figure 7 shows the critical diameter as a function of dry particle diameter based on the fraction of soluble matter in the droplets. This was calculated from the hygroscopic growth measurements using the tandem differential mobility analyser (TDMA).

The hygroscopic properties as measured using TDMA were in fairly good agreement with the fraction of ionic compounds, as determined with ion chromatography analyses and gravimetric weighing of impactor samples during this campaign (Berg et al., 1998). This implies that mainly inorganic species were responsible for the growth. These hygroscopic growth measurements are related to 90% relative humidity. However as the relative humidity increases and the fog forms, some additional aspects have to be considered in relation to activation:

(a) Dissolution of slightly soluble organic compounds by the more diluted solutions

(b) Change of the surface tension by presence of organic compounds in more diluted solutions

(c) The effect of volatile ionic solutes

The first two aspects are effects that the TDMA monitors when determining the hygroscopic growth at 90% relative humidity (RH), however the critical diameter is attained at about 100%, when the droplets are more dilute. Recent modelling results showed that slightly soluble organic compounds may remain undissolved in the concentrated solution at 90% relative humidity and only enter the solution of the more diluted droplets when the fog forms (Shulman et al., 1996). Recent measurements at the sampling location used in these studies have found that organic species constituted 25–50% (by mass) of the total dissolved compounds in fog water and a major fraction of these consisted of high polarity macromolecules in the 10000 AMU region (Fuzzi and Zappoli, 1996). These species could either be dissolved, or partly dissolved at 90% relative humidity (and thus be accounted for in the TDMA measurements), or enter the solution when the fog forms from the diluted droplets. The result of this behaviour is an increase of the critical diameter.

The droplet growth is also affected by the surface tension of the droplets. Capel et al. (1990) found that the surface tension of fog water depended on the concentration of dissolved organic matter. At low concentrations, below 100 mg/l, the surface tension was similar to that of pure water, but was approximately 80% of that value in more concentrated solutions. The net result of a decreased surface tension is an increased critical diameter.

The uncertainty in detailed knowledge concerning organic compounds is probably not of great significance. The influence on condensational growth (and hence, the critical diameter) by organic compounds is very low, if the soluble fraction is more than 10% (Lemmel and Novakov, 1995).

The third aspect is the possible influence of the measuring technique. The TDMA (and also the DAA) samples wet droplets, which are dried in the instrument and during this process volatile soluble species, e.g. HNO_3, can evaporate. The amount of soluble material in the droplet could therefore have been greater than that measured by TDMA, resulting in a larger critical diameter for the dry residue particle measured.

When the DAA data are related to the critical diameter according to TDMA measurements in Figure 7, it can be seen that no activated droplets appear in case B, while a shallow activation can be seen in case A. Thus, for the latter case, particles smaller than 0.55 µm (critical droplet diameter, 8 µm) formed unactivated droplets, while larger ones formed activated droplets (at least up to 0.9 µm dry diameter).

The interpretation of the dependency of the ambient diameter on the dry residue diameter related to the droplet activation process, depends on how the hygroscopic properties are described. With the assumption that the hygroscopic properties, as measured by

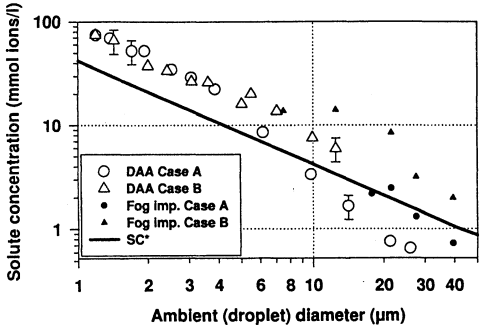

Figure 8: The fog droplet solute concentration as function of ambient (droplet) diameter measured by DAA and size resolved fog droplet impactors. The line (SC*) represents the solute concentration at the critical droplet diameter for activation. The bars show one standard deviation of the error and the errors are in the same range for all presented droplet diameters.

TDMA, can be extrapolated to the conditions prevailing in a diluted fog droplet, a weak activation sometimes occurred in the fog studied, for the droplets nucleated on the largest accumulation mode particles. Dissolution of additional material in the diluted state, a reduced droplet surface tension and the effect of evaporating soluble species, all tend to increase the critical diameter for a given residue size. The fog can for most of time during this campaign therefore be classified as consisting of unactivated droplets, while it is not clear from these measurements, if the few periods when the critical diameter, calculated from TDMA-measurements, was exceeded, actually was a result of activation.

3.5 Fog Droplet Solute Concentration

A large fraction of gas-to-particle conversion in the atmosphere can be attributed to fog and cloud droplet reactions. Chemical reactions in fog and cloud droplets are assumed to be strongly dependent on the solute concentration in the droplets, for instance pH-dependent reactions (Twohy et al., 1989). Theoretical considerations and model calculations show that the droplet solute concentration is also strongly dependent on droplet size (Ogren and Charlson, 1992).

The size dependent solute concentration (solute = dissolved soluble species) in droplets, for cases A and B, are presented in Figure 8 in relation to the critical solute concentration for activation according to the Köhler equation. The dry diameter associated with the ambient diameter, as measured using DAA, together with the amount of soluble species in the particles calculated from the hygroscopic properties measured by TDMA, have been used to calculate the solute concentration:

$$SC = \left(\frac{D_p}{D_d}\right)^3 \cdot \varepsilon \frac{i\rho}{m_s} \quad \text{[mole ions / l]} \qquad (3.1)$$

where SC = solute concentration, D_p = dry particle diameter, D_d = ambient (droplet) diameter, ε = soluble fraction (by volume) calculated from TDMA measurements, i, ρ and m_s = number of ions per molecule, density and molecular mass of the solute.

Figure 8 also shows the solute concentrations measured by the size resolved fog droplet impactors for the two case studies (Laj et al., 1998). The two methods found similar overall behaviour, with both showing the decrease with increasing diameter and the magnitude of the decrease. However the fog droplet impactors found in most cases higher solute concentrations. This can partly be explained by the DAA data being based on measurements of the ambient size and dry residue size. Inevitably, some volatile compounds can escape the particle during the diffusion drying process of the droplets in the instrument. This could to some degree affect the solute concentration. Part of the difference may also be explained by the measurement errors of the two methods. The size dependent chemical composition of fog droplets, during this campaign, are described and discussed in more detail by Laj et al. (1998).

It can be seen in Figure 8 that the solute concentration of the two cases show same behaviour up to 4 µm in diameter, while for larger droplet diameters the solute concentration is much lower for case A. It can also be seen that both measuring methods show results that are below the critical solute concentration (based on the Köhler equation and the surface tension of pure water) for large droplet sizes in case A, while all droplets remain unactivated in case B.

The solute concentration was found to be strongly size dependent, rapidly decreasing with increasing droplet size. In case A, this decrease was by more than a factor of 100 in the droplet size region 1–40 µm, but somewhat less in case B. The decreasing solute concentration with size is expected for unactivated droplets in the equilibrium state, while the opposite dependence is expected for large growing droplets, where the dynamics of the growth prevents the droplets from reaching their equilibrium size in the time available for the growth, see Chapter 4.

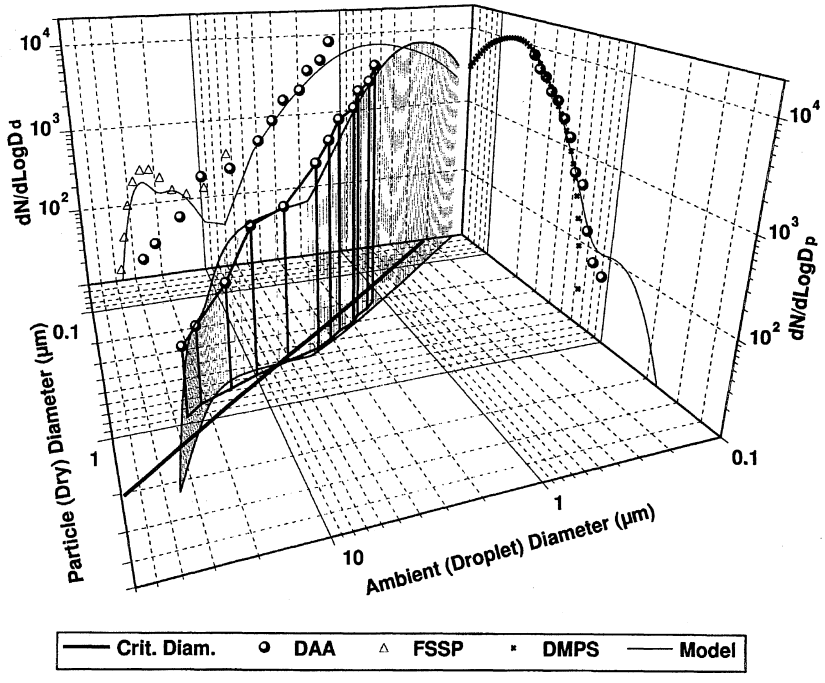

Figure 9: The number concentration as function of ambient (droplet) diameter and dry particle diameter as measured by the DAA and obtained from the closed parcel model. The bold line shows the critical diameter of droplet activation. The number concentration is given in the form $dN/d\log D_p$; where D_p is the dry particle diameter. The projection to the right shows $dN/d\log D_p$ as function of D_p obtained from the DAA and the DMPS together with the line which shows the particle size distribution used as input to the model. The projection to the left shows $dN/d\log D_d$ as a function of D_d; where D_d is the ambient (droplet) diameter; measured by the DAA and the FSSP together with the model results. The aerosol mass load was 50 µg m^{-3}; the LWC 0.4 g m^{-3} and the constant c was 10^{-7} s^{-2}.

4 Modelling of the Fog Microstructure

In this section the experimentally observed microstructure of the fog will be related to that expected from modelling studies. The latter is obtained from a closed parcel cloud model, where the fog formation and development is simulated. The aim is not to describe the fog in all its details, because some important experimental parameters are missing. It is very difficult to retrieve the history of the air mass observed at the experimental site due to the advection. This implies that the variations in observed parameters (e.g. LWC) do not necessarily reflect the evolution of the fog since they could also be indicative of spatial variations. The emphasis will therefore be placed on exploring the main features of the fog microstructure. In the first sub section the model will be related to experimental data and in the following sub sections, the effects of air mass cooling rate, aerosol mass load and the ageing of the fog will be investigated.

4.1 Model Related to Measurements

In the previous section it was shown that most of the time the fog consisted of unactivated droplets. During a short period of the campaign activation possibly occurred. The sub section will concentrate on this period, because we will show in the following that a clear example of a fog consisting of only unactivated droplets can easily be obtained from the model. The fog started at 20.30 h on the 13th November and reached a LWC of 0.5 g m^{-3} after 1 h. The value dropped to 0.1 g m^{-3} . Half an hour later the LWC had returned to a high level, which then persisted for

several hours. The DAA measurements showed that activation possibly occurred, both before and also two hours after the minimum in the LWC. DAA data from four 15 min. measurement periods, with each being used to measure three different residue sizes, covering the time period 22.20 - 23.20 h (case A), will be compared with the results from modelling. These measurements were thus taken in the time period when the LWC had just returned to the higher level. As pointed out above, variations in LWC can be caused by variations in both time and space due to advection. The horizontal wind speed was around 3 m s^{-1}, implying that advection could be a reason for the variations in the LWC. Nevertheless, the temporal LWC variations were similar to those used in the model. The time period covered by the measurements was in this time frame, in the region where the effect from the rate of temperature decrease, during the onset of the fog, has begun to decline according to modelling. The ageing of the fog will be discussed in Section 4.4. The modelling results obtained are compared with the experimental data from the DAA, FSSP and DMPS in Figure 9. The dry particle size distribution of the DAA and the DMPS was used as input for the model, to describe the particle size distribution in the sub micrometer diameter region. The discrepancy between the two instruments above 0.5 μm dry diameter was due to the interstitial inlet ambient cut-off diameter of 5 μm used for the DMPS measurements, see the dry particle size distribution projected in Figure 9. The upper sub micrometer and super micrometer dry size distribution was estimated by weighing together the data from the DAA, FSSP and the size-resolved fog impactors, as described in Section 3.2.

The model was started at a saturation ratio of 0.998 and the temperature was decreased isobarically to produce supersaturation. Several different rates of temperature decrease were used in the modelling. For the case shown in Figure 9, the temperature gradient was -0.17 mK s^{-1} (depends primarily on the constant c) when the maximum saturation ratio (1.00027) was reached. This approximately corresponds to an updraught velocity of 0.02 m s^{-1} in an adiabatically rising air mass. The modelling results displayed shows the situation 85 min after the start of the model, when 90% of the LWC has formed. Good agreement between model and measurements, in the relation between ambient size and dry particle size up to 0.7 μm dry diameter can be seen (the 3D part of Figure 9), where the modelled sizes follow those measured, in the region with unactivated droplets (small diameters) and turn over the critical diameter of activation (the bold, solid line). For the two largest dry particle sizes measured, the model somewhat underpredicts the ambient size. Figure 9 also shows that the largest particles remain unactivated according to the model, although their critical supersaturation with respect to activation was exceeded by the fog. This can be explained by limitations caused by the rate of droplet growth. The droplet diameter growth rate depends, to the first approximation, inversely on the droplet diameter. Hence the larger the critical diameter, the longer the time required for the growth to reach activation.

The projected ambient size distribution of Figure 9 ($dN/d\log D_d$) shows good agreement between the model and the DAA results, up to 4 μm and with the FSSP to large diameters ($D_d > 10$ μm). The DAA is not expected to reproduce the mode of large droplets because these are nucleated on super micrometer dry particles which were not measured, see Section 3.3. The dip of the ambient size distribution around 7 μm in the model was caused by droplet activation. It will be shown below that the shape of the size distribution in that region can vary substantially with time and dynamics of the fog. Overall it can be seen that most of the major characteristics of the fog were reproduced by the model, i.e. most of the dry/ambient size relations, the continuum from small to super micrometer droplets and the small mode of very large (25 μm) droplets.

4.2 Influence of the Rate of Temperature Decrease

The rate of temperature decrease during the fog formation was varied in the model by one order of magnitude, by varying the constant c between 10^{-6} – 10^{-8} s^{-2}, while keeping the dry particle size distribution and the final LWC of the fog constant (0.4 g m^{-3}). The relationships between ambient diameter and dry particle diameter and the droplet size distribution, when 90% of the final LWC had been produced by the five model runs at different temperature gradients are shown in Figure 10. The 90% level was chosen as one reference point in the presentation of the modelling results, where features of somewhat longer duration compared to earlier stages in the fog formation, can be discerned. The development with time of the fog is dealt with in Section 4.4. It can be seen that the model produces more activated droplets where the rate of temperature decrease was the greatest. The activation went further down in dry particle diameter the stronger the decrease. It can also be seen that the larger super micrometer particles did not exceed the critical diameter of activation because of the

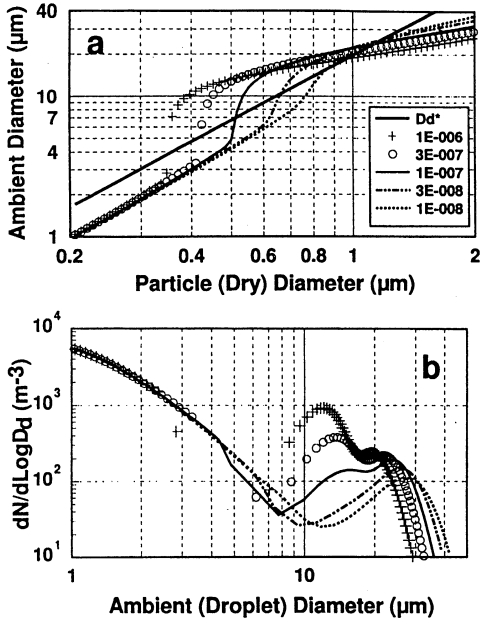

Figure 10: Microphysical characteristics from simulations with varied temperature gradient during the formation of the fog. The values of the constant c ($10^{-6}...10^{-8}$ s^{-2}) correspond to maximum rates of temperature decrease of -0.56; -0.31; -0.18; -0.10 and -0.056 mK s^{-1}. See also Figure 1. The graphs show the situation when 90% of the final LWC of the fog was formed. The aerosol mass load was 50 µg m^{-3} and the final LWC 0.4 g m^{-3}. a) The ambient (droplet) diameter as function of dry particle diameter. The bold line shows the critical diameter of activation. b) The droplet size distribution as a function of ambient diameter.

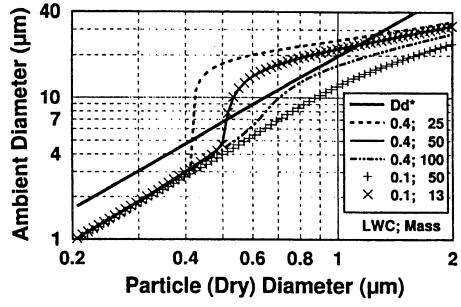

Figure 11: The ambient (droplet) diameter as a function of dry particle diameter for various aerosol mass loads (in µg m^{-3}) and LWC (in g m^{-3}). The value of the constant c was 10^{-7} s^{-2}. The bold line (Dd*) shows the critical diameter of activation.

limitation in the rate of growth, although the largest droplets were nucleated on the largest particles. In Figure 10a it can also be seen that almost no activation occured at the lowest rate of the temperature decrease during fog formation. Thus, the most commonly observed structure of the fog in this campaign, i.e. that of a fog without activated droplets, is readily modelled using a sufficiently low rate of change in the temperature.

The resulting droplet size distributions for different rates of temperature decrease during fog formation are shown in Figure 10b. It can be seen that the distribution varies strongly with this rate. The common feature of all distributions is that of a mode at large droplet diameters of low number concentrations. These droplets were formed on the super micrometer particles. The main difference between the cases appear around 10 – 15 µm diameter, where a second droplet mode appears. This mode becomes more prominent as the rate of temperature change increases, and by comparing with Figure 10a it can be seen that the major part of this mode consists of activated droplets. It can also be seen that a significant gap develops for the fastest fog formation cases, in the distribution between the activated droplets and the smaller unactivated droplets, which were formed on small particles. Thus, the activation process makes a very strong impression on the droplet size distribution. For the most rapid rates of temperature decrease during fog formation, the droplet number concentration was very much higher in the mode of activated droplets compared to the mode of droplets nucleated on the supermicrometer particles.

4.3 The Effect of the Aerosol Mass and the LWC of the Fog

The aerosol mass present in the developing fog was varied by a factor of 4 (25 - 100 µg m^{-3}; the total mass of ammonium sulphate and/or nitrate) in three modelling cases. The previous model results have used a mass load of 50 µg m^{-3} and the experimentally measured values (DAA and estimates of super micron particles, see Section 3.2) were in case A, 70 µg m^{-3} and in case B, 85 µg m^{-3}. The size distribution of the dry aerosol particles was held constant and the same as in the sub sections above and the value of the constant c used was 10^{-7} s^{-2}. Figure 11 shows the relation between the ambient and the dry particle diameter when the LWC reached 90% of its final level. The aerosol mass load strongly influenced the microstructure of the fog. From the results obtained it would appear that a doubling of the mass

load from 50 μg m^{-3} does not lead to the formation of activated droplets. Thus, similarly to a slow temperature decrease during fog formation, a high mass load can also produce a fog without activated droplets. At lower mass loads, activated droplets are formed on smaller particles. It can also be seen that a decreased aerosol mass load led to generally larger droplets for a given particle dry diameter, including the super micrometer dry particle diameter region. This is to be expected because the LWC is then divided by fewer droplets.

The LWC of a fog is an important parameter in conjunction with the aerosol mass load. In the modelling presented thus far the LWC was 0.4 g m^{-3} and the experimental (by FSSP) values were in case A, 0.46 g m^{-3} and in B, 0.38 g m^{-3}. These are high values for fogs, compared to those commonly reported of below 0.1 g m^{-3} (Pruppacher and Klett, 1980). The case presented in Figure 9 was from the period with the highest LWC, during the present campaign (case A); a value of 0.1 g m^{-3} would be more typical. In Figure 11 it can be seen that by reducing the LWC to this value and keeping the aerosol mass load at 50 μg m^{-3} no activated droplets are formed. To further investigate the relation between aerosol mass load and LWC, the aerosol mass load was decreased with the same factor as the LWC to 13 μg m^{-3}. In Figure 11 it can be seen that the ambient sizes, as a function of dry particle size, are almost identical to the case with the same relation between the LWC and the aerosol mass load, i.e. 0.4 g m^{-3} and 50 μg m^{-3}. Thus, the effect of the aerosol mass load inter-related with the LWC of the fog and together they strongly influence the microstructure of the fog.

4.4 The Ageing of the Fog

So far the modelling has been presented as "snap shots" for given conditions in the fog, in order to present the effect of some parameters. However, each modelling procedure describes the formation and evolution of the fog for a given set of input parameters. The microstructure of the fog varies with time according to the model and the evolution has been followed for about 3 h. It can be argued whether it is realistic to follow the fog for such a long time with a closed parcel model. The distribution of the water between the droplets may be affected by mixing processes (Wobrock et al., 1998) and occasionally by drizzle formation (Wendisch et al., 1998). At long fog times gravitational settling of the droplets may affect the microstructure, e.g. a 25 μm droplet fall 70 m during one hour. Hence, the large droplets will be lost

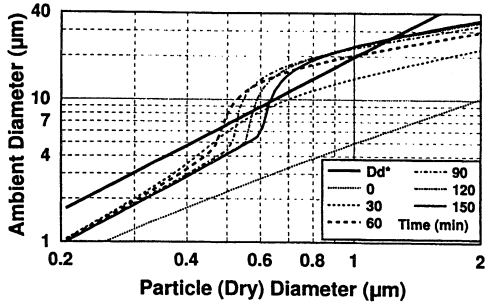

Figure 12: The ambient (droplet) diameter as a function of dry particle diameter related to the time from the start of the model for the case aerosol mass load was 50 μg m^{-3}; the LWC 0.4 g m^{-3} and the constant c was 10^{-7} s^{-2}. The bold line shows the critical diameter of activation.

from the air mass unless a thick fog layer above can replace them. Keeping these complications in mind, it is still interesting to study the intrinsic dynamics of the droplet growth, which are related to the fog dynamics and, in particular, the effect of the size-dependent water vapour pressure at the droplet surface.

In all the model computations the fog formation was described by an isobaric temperature decrease using the expression given in Section 2.3. This means that the liquid water of the fog is produced at the beginning, with a rate which varies with the constant c, thereafter the temperature and hence the LWC remain at a constant level. Figure 12 shows an example (the same case as shown in Figure 9) on how the ambient size dependency on the dry particle size changes with time, from the start of the model at the saturation ratio 0.998. The almost straight line at small ambient diameters show the initial conditions. Fog droplets which have nucleated on dry particles with diameters around 0.6 μm, approached activation after 30 min and after 60 min, activated droplets have formed on dry particles with diameters in the size region 0.49 – 1.0 μm. As time passes, the dry size region with activated droplets shifts towards larger diameters and after 90 min the dry size diameters 0.53 - 1.1 μm were the sites of the activated droplets. This means that some droplets (those nucleated at dry sizes 0.49 – 0.53 μm) are de-activated in the fog at the same time as new activated droplets are formed on the dry particles in the 1.0 – 1.1 μm size region. The droplet size distribution from almost the same time (80 min) is shown in Figure 10b (the case of $c = 10^{-7}$ s^{-2}) where 90% of the LWC had formed. As the fog persists, with a slow convergence to zero rate

of liquid water production, the redistribution of the water from the activated smaller droplets to the large droplets, which have nucleated on the largest particles, continues.

The redistribution of the fog water can be better understood by studying the time required for fog droplets to react on a change of relative humidity. Hänel (1987) deduced an expression which characterises the response time of an equilibrium sized droplet to a step change in the saturation ratio (S). This can be obtained by relating the given step size to the rate of change in the saturation ratio at the droplet surface (S_a):

$$\tau = \frac{S - S_a}{\frac{dS_a}{dt}} = \frac{S - S_a}{\frac{dS_a}{dD_d}\frac{dD_d}{dt}} = \frac{D_d}{g\frac{dS_a}{dD_d}} \qquad (4.1)$$

where

$$\frac{dD_d}{dt} = \frac{g(S - S_a)}{D_d}$$

dS_a/dD_d can be obtained from the Köhler equation and g is a function of several parameters (Pruppacher and Klett, 1980). It can be seen that the time is independent of the step size in relative humidity, implying that the quantity can be used as a measure of the response time at given conditions. The droplet attaines the new equilibrium state after approximately 5τ, according to Hänel (1987). This can be used as a measure of the time required for equilibrium droplets to adjust to changes in relative humidity. The values obtained for five initial conditions (90, 99, 99.9, 100 and 100.005 % relative humidity), together with droplet size for dry particle diameters 0.2, 0.5 and 1 μm, consisting of 50% $(NH_4)_2SO_4$ and 50% insoluble material are presented in Table 4. It can be seen that the time to reach the new equilibrium depends strongly on the initial relative humidity, droplet size and the dry particle size. Below 99% relative humidity the time is 5 s or less for particles smaller than 1 μm. Close to saturation the time required becomes significantly longer and of the same order of magnitude, or longer than the time evolution period studied by the fog model. The 1 μm particles require about 10 h to reach the new equilibrium state at 0.05% supersaturation. For equally sized droplets it can also be seen that a droplet containing a less concentrated solution requires a longer time to adjust than one containing a more highly concentrated solution, for example compare the 0.5 μm particle at 0.05% supersaturation with the 1 μm particle at -0.1%, see Table 4. This is caused by the very weak dependency

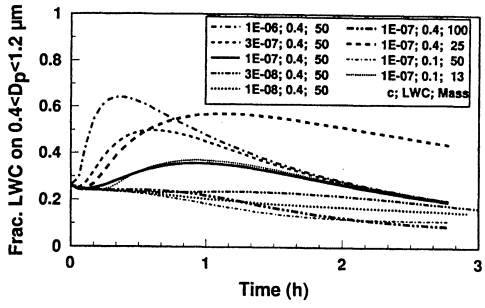

Figure 13: The fraction of the fog LWC carried by droplets which nucleated on particles which in the dry state belong to the size region 0.4–1.2 μm ("activation ratio") as a function of the time from the start of the model. The temperature gradient during the formation of the fog (in terms of the constant c (s^{-2})); the aerosol mass load (μg m^{-3}) and the LWC (g m^{-3}) was varied. See the caption of Figure 10 for interpretation of the constant c.

of the water activity on droplet size for diluted solutions, i.e. larger changes in droplet size is required as the water activity approaches 1. These results imply that the largest particles studied here cannot follow the development of the relative humidity during the fog formation and that their reaction to fluctuations is slow after the fog has formed.

Almost all the activated droplets are nucleated on dry particles within the size region 0.4 – 1.2 μm, see Figures 10a, 11 and 12. In order to obtain an overview different simulations, with respect to the redistribution of the water between the droplets, the ratio of the integrated liquid water associated with that dry particle size region to the total LWC, were computed as a function of time from the start of the model (the "activation ratio"). Hence, in these simulations, which all used the same dry particle size distribution (but not the same number concentration), a high value of this ratio means that a large fraction of the LWC was associated with the activated fog droplets. The results of these simulations are shown in Figure 13 for various rates of temperature decrease, aerosol mass loads and LWC. It can be seen that a high mass load, a low LWC, or a low rate of temperature decrease produces a low "activation ratio" during the time covered by the simulations. Thus, no or very limited activation takes place. For greater rates of temperature decrease, higher LWC or lower aerosol mass loads, the fraction of the LWC associated with activated droplets was substantial at the beginning of the simulations and drops off as the fog develops. In the example shown in Figure 12 the maximum in the "activation ratio" was after approximately 60 min

Table 4: The droplet diameter (D_d) and time required to adjust to a new equilibrium state (5τ) after a step change in relative humidity for three particle diameters (D_p) as a function of water vapour supersaturation. The particle composition is 50% ammonium sulphate and 50% insoluble matter.

Dp (μm)	0.2	0.5	1	0.2	0.5	1
Supersat. (%)	D_d (μm)			5τ (min)		
-10	0.32	0.80	1.61	9.3E-05	4.7E-04	1.8E-03
-1	0.60	1.59	3.25	2.7E-03	0.019	0.081
-0.1	0.95	2.94	6.44	0.031	0.47	2.7
0	1.12	4.44	12.6	0.081	4.7	105
0.05	1.33	6.23	20.2	0.24	49	5390

and reached 90% of the final LWC 80 min after the start of the model. In cases with still higher rates of temperature decrease and an ionic mass load of 50 μg m^{-3}, even higher values of the "activation ratio" were attained at the beginning of the simulations, but after approximately 1.5 hour most of the water had transferred from the activated droplets to the larger droplets nucleated on the super micrometer particles.

A reduction of aerosol mass load for a given LWC leads to a longer life-time of the activated droplets, compare for example a mass load of 25 μg m^{-3} with that of 50 μg m^{-3} at 0.4 g m^{-3} LWC, see Figure 13. Again, a reduction of both the aerosol mass load and the LWC by a factor of 4 (from 50 to 13 μg m^{-3} and 0.4 to 0.1 g m^{-3}) leads to an almost identical dependence on time of the activation ratio for the two cases, see Figure 13. This implies that the rate of the re-distribution of the fog water, from the activated droplets, to the droplets nucleated on the largest particles, is strongly dependent on the relation between the LWC and aerosol mass load and hence the degree of dilution of the droplets. This can be further explained using the results presented in Figure 11. It can be seen from this that a reduced aerosol mass load for a given LWC leads to overall larger droplets. The activated droplets were in the size region of 13–28 μm for the case at 25 μg m^{-3} mass load, compared with 10 – 23 μm for the example with 50 μg m^{-3}. In addition the unactivated droplets nucleated on the super micrometer dry particles were significantly larger in the former example. For unactivated droplets the growth leads to an increase of the water vapour pressure at the droplet surface (p_a), while it decreases for activated droplets. This directly reduces the rate of redistribution of water to the large unactivated droplets because of the reduction of the difference between the two types of droplets, in the expression ($p_{inf} - p_a$), where p_{inf} is the water vapour pressure far away from the droplet, which is almost directly proportional to the growth rate (positive or negative) of the droplets. As a consequence it takes longer time for the large unactivated droplets to consume the water available, when the aerosol mass is reduced for a given LWC.

5 Discussion

The microstructure of the fogs in the present study show in some respect the same picture as in previous fog studies, but a major discrepancy is the conclusions regarding activation and scavenging. The fogs studied differs though significantly from what have been observed in clouds.

The results from this study shows that most of the time the fog consisted of unactivated droplets. Discussions of scavenging by activation are therefore not relevant. Previous fog studies at the same location (Noone et al., 1992) based on the counter-flow virtual impactor (CVI) defined the ambient droplet diameter 5 μm as the minimum size of the fog droplets, while those smaller were classified as interstitial aerosol particles. In the present study such a criterion would lead to that the limiting size would be in a continuous distribution. It is not clear if the scavenging presented in Noone et al. (1992) are a real effect or if it could be an effect of the measuring technique used, because no measurements regarding the activation status of the fog droplets were made during that campaign.

The difference between the present fog study and previous cloud studies can be demonstrated by comparing the relation between ambient droplet diameter and dry particle diameter from a typical case of a study of orographic clouds (Martinsson et al., 1997) with a typical case (case B) from the present fog study, see Figure 14. It can be seen how the activation in the orographic cloud resulted in cloud droplets which were up to a factor of 10 larger than the critical diameter of activation. Hence, a mode of activated droplets formed which in terms of ambient size, were separated from the interstitial aerosol

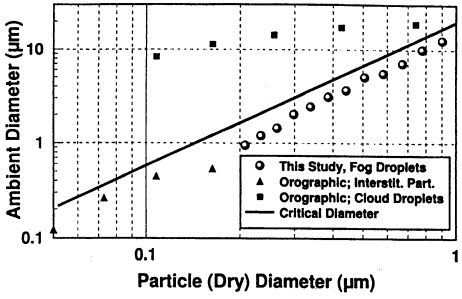

Figure 14: The relation between ambient and dry particle diameter measured with the DAA. A typical case from a study of orographic clouds (Martinsson et al., 1997) compared with a typical case from the present fog study. The occurrence of two curve symbols for some dry particle diameters in the cloud case was caused by that a fraction of those particles served as cloud condensation nuclei while the remainder of them were interstitial aerosol particles. The critical diameter is a representative line which is close to the lines for both the fog and the cloud experiment.

particles. Differences between the results from the present fog study and the orographic cloud study are that the clouds usually formed with a significantly faster temperature decrease (varied between -3 and -20 mK s^{-1} as deduced from the updraught conditions of the air mass) than the fogs presented in Section 4. The aerosol concentration was generally lower in the orographic clouds, while the LWC was higher. Another important difference is found in the duration of the two systems. While the orographic cloud commonly produce supersaturation in a given air mass for a relatively short time period (tens of minutes), the fog may persist several hours or more. The study of orographic clouds showed also that almost all the cloud water was associated with activated droplets in a mode at 10 – 15 µm diameter which was formed on sub-micrometer particles. That mode was well separated from the interstitial aerosol, see Figure 14. Particles of dry sizes down to 0.1 µm served as cloud condensation nuclei. The results from the present fog study showed a small mode with large droplets which contained a large fraction of the fog water. These droplets were associated with particles that are super micrometer, in the dry state.

Fog droplet distributions similar to the ones found in the present study has been observed in previous studies (Pruppacher and Klett, 1997). These studies show continuos fog droplet distributions, i.e. no gap in the distribution as could be seen in for example the study of orographic clouds mentioned above, see Figure 14. Model results of the fog, presented in Section 4, also show that a continuos distribution will be obtained if the droplets remain unactivated or just "slightly" activated, see Figure 10b.

The results from this experiment show that the fog droplet solute concentration has a strong dependence with droplet size. This has also been observed in a previous study (Ogren et al., 1992) at the same sampling location. They found the same size dependency, i.e. decreasing solute concentration with increasing droplet diameter, and the results from that experiment is in good agreement with the present study. This indicates that the fogs in the previous study at the same location (Noone et al., 1992; Ogren et al., 1992) had a similar microstructure as the fog in the present study.

Other experimental and modelling studies of size dependent solute concentration in fogs and clouds (Noone et al., 1988; Ogren et al., 1989; Pandis et al., 1990; Ogren and Charlson, 1992; Martinsson et al., 1997) show also a strong dependence of solute concentration on droplet size. In Pandis et al. (1990) fog development was studied with a model and the results show a decreasing solute concentration with increasing droplet size. Noone et al. (1988) and Ogren et al. (1989) present experimental studies of droplets in clouds. Their results show an increasing solute concentration with increasing droplet size. Ogren and Charlson (1992) were dealing with modelling of cloud droplets. Their results show that droplets at time for activation, i.e. still at equilibrium conditions, have a decreasing solute concentration with increasing droplet size and that activated cloud droplets have an increasing solute concentration with increasing droplet size. Martinsson et al. (1997) presents experimental and modelling results of cloud droplets and the results show an increasing solute concentration with increasing droplet size for activated droplets while decreasing for the small, interstitial aerosol particles. Thus, the clouds commonly produce a reversed size dependency of the solute concentration compared to what has been observed and modelled for fogs.

Several factors affect the droplet size dependency of the solute concentration. Some basic features can be highlighted with the fog model results presented in Section 4. Figure 15 shows six "snap shots" from five fog developments modelled, i.e. the situation when 90% of the LWC was formed is displayed except for the curve marked with (*) which shows the situation approximately 80 min later (the two last entities of the Figure legend were taken from the same

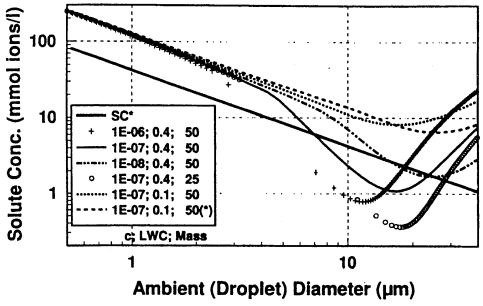

Figure 15: The solute concentration as a function of fog droplet diameter from simulations after 90% of the LWC was formed; except the simulation marked(*). That comes from the same simulation as the simulation above in the legend; but shows the solute concentration at the end of the simulation (approximately 80 min later). The temperature gradient during the fog formation was varied (c (s^{-2})) together with the LWC (g m^{-3}) and the aerosol mass load (μg m^{-3}). The bold line shows the solute concentration at the critical diameter of activation (SC*). The curve symbols relate to the actual size groups used in the model; which were equally spaced by a factor of approximately 1.033 in the dry state. The variable spacing as a function of ambient diameter is a consequence of the dynamics of the growth.

modelling case). Three particularly interesting features of the size dependency can be pointed out from Figure 15. All the modelling cases result in approximately the same behaviour for small droplets with a decreasing solute concentration with droplet size, some of the cases show a gap in the distribution at intermediate droplet sizes and the solute concentration increases with the size for the largest droplets. The resemblance of the cases at small droplet diameters can be attributed to that the droplets have assumed their equilibrium size. The small difference that can be observed is caused by slight differences in the relative humidity. It can also be seen that the upper limit of the equilibrium size region varies from below 3 μm diameter for the case with the fastest temperature decrease ($c = 1 \times 10^{-6}$ s^{-2}) to the order of 20 μm for the case marked with an asterisk. (The slope of the equilibrium solute concentration curve closely resembles that of the critical solute concentration well below the activation point where it turns towards that curve, see e.g. the curve of the $c = 1 \times 10^{-8}$ s^{-2} case.) Those cases where activated droplets formed (i.e. a solute concentration lower than the critical solute concentration) is characterised by that a gap develops in the droplet size distribution. For e.g. the case with 25 μg m^{-3} aerosol mass load very few droplets are found in the size region 3 – 18 μm, implying that the fog from practical point of view consists of two kinds of droplets: the small unactivated with decreasing solute concentration with size and the large droplets where the solute concentration increases with size. It can be seen that the latter size region includes activated droplets up to approximately 27 μm, while those larger are unactivated. Nothing dramatical happens around the activation line in this size region. The difference between the droplets, except for the size, is that the vapour pressure at the droplet surface decreases with increasing droplet size, which influence the ageing of the fog, see Section 4.4. None of these droplets are of equilibrium size, implying that they are either growing or shrinking at any given relative humidity. From the case with the LWC 0.1 g m^{-3} it can be seen that no activation is required in the fog for the occurrence of a droplet size region where the solute concentration increases with size. These droplets are still in the growing phase, as can be seen by comparing the two curves from that case which are separated in time by approximately 80 min. Such a dis equilibrium is caused by insufficient growth rate for the large droplets (which were nucleated on large aerosol particles) to reach the equilibrium size.

The closed parcel fog modelling shows the intrinsic features of droplets growing by vapour diffusion to the droplets. From this it was found that the fog consists of two kinds of droplets, those of equilibrium size and those which are not at equilibrium. The droplets at equilibrium appear at the small droplet size end, where the solute concentration decreases with droplet size. The large droplets were found to be at dis-equilibrium with respect to droplet size and the solute concentration increasing with size. Such droplets can be activated or unactivated. Depending on several factors, the transition between the two regimes can be smooth or be characterised by a gap in the distribution caused by droplet activation and the droplet size where the transition takes place is strongly dependent on the conditions prevailing in the fog.

6 Conclusions

In this study of fog formation in a polluted region of northern Italy it was found that the fog droplet size distribution was continuos in the size region 1 – 47 μm without any gaps generated by the droplet activation process, which has been observed in clouds. This means that the activation cannot be studied by relating to any fixed droplet diameter. In this study the droplet aerosol analyser (DAA) was used to determine connected ambient (droplet) and dry residue

sizes. By relating these quantities to each other it was found that the fog consisted of unactivated droplets or droplets possibly larger than the critical diameter for activation (according to the Köhler equation). The solute concentration of the fog droplets was generally higher than observed in a hill cap cloud and it decreased with increasing dry residue (or droplet) diameter. This reversed dependency compared with the "normal" situation in a cloud can be explained by the Kelvin effect for unactivated droplets and by the low growth rate of those droplets possibly activated caused by the large size of their condensation nuclei.

The most common situation thus was that the fog consisted of only unactivated droplets with a continuous droplet size distribution. By modelling, it was shown that a low rate of temperature decrease during fog formation and a high aerosol mass load in relation to the LWC of the fog result is such a fog. Also ageing of the fog tends to produce a fog without activated droplets from a fog which initially contained activated droplets, by redistribution of the fog water from the activated droplets to larger unactivated droplets. The effect of the aerosol mass load was found to be particularly influential. These measurements of fog characteristics were undertaken in a polluted area in Northern Italy. Bearing in mind the very strong influence of the aerosol mass load on the fog it can be expected that fogs formed in an area with a lower aerosol burden might exhibit a significantly different microstructure. Hence, the results presented here represent a case of fog formation and development in a polluted region.

Acknowledgement

We would like to thank our colleagues at FISBAT-institute for their work associated with hosting this campaign. We would also like to thank A. Andreoli, D. Correggiari, F. Fanti and L. Tarozzi for assistant during the field operations. The funding of this research by the Swedish Natural Science Research Council and by the European Commission (Contract EV5V-CT93-0314) is gratefully acknowledged.

References

Berg O.H., Swietlicki E., Frank G., Martinsson B.G., Cederfelt S.-I., Laj P., Ricci L., Berner A., Dusek U., Galambos Z., Mesfin N.S., Yuskiewicz B., Wiedensohler A., Stratmann F. and Orsini D., 1998: Comparison of observed and modeled hygroscopic behavior of atmospheric particles. Contr. Atmos. Phys. **71**, 47–64.

Capel P.D., Gunde R., Zürcher F. and Giger W., 1990: Carbon speciation and surface tension of fog. Environ. Sci. Technol. **24**, 722–727.

Cederfelt S.-I. and Martinsson B.G., 1996: A charging unit for droplet aerosols. Internal report no. LUTFD2/(TFKF-3080)/1-8(1996).

Cederfelt S.-I., Martinsson B.G., Svenningsson B., Frank G., Hansson H.-C., Swietlicki E., Wiedensohler A., Wendisch M., Beswick K.M., Bower K.N., Gallagher M.W., Pahl S., Maser R. and Schell D., 1997: Field validation of the droplet aerosol analyser. Atmos. Environ. **31**, 2657–2670

Chen J.-P., 1994: Theory of deliquescence and modified Köhler curves. J. Atmos. Sci. **51**, 3505–3516.

Fuzzi S., Facchini G., Orsi G., Lind J.A., Wobrock W., Kessel M., Maser R., Jaeschke W., Enderle K.H., Arends B.G., Berner A., Solly I., Kruisz C., Reischl G., Pahl S., Kaminski U., Winkler P., Ogren J., Noone K.J., Hallberg A., Fierlinger-Oberlinninger H., Puxbaum H., Marzorati A., Hansson H.-C., Wiedensohler A., Svenningsson I.B., Martinsson B.G., Schell D. and Georgii H.W., 1992: The Po Valley fog experiment 1989: An overview. Tellus **44B**, 448–468

Fuzzi S. and Zappoli S., 1996: The organic component of fog droplets. 12th International Conference on Cloud and Precipitation: Proceedings - Vol. 2, 1077–1079

Fuzzi S., Laj P., Ricci L, Orsi G., Heintzenberg J., Wendisch M., Yuskiewicz B., Mertes L., Orsini D., Schwanz M., Wiedensohler A., Stratmann F., Berg O.H., Swietlicki E., Frank G., Martinsson B.G., Günther G., Dierssen J., Schell D., Jaeschke W., Berner A., Dusek U., Galambos Z., Kruisz C., Mesfin S.N., Wobrock W., Arends B. and ten Brink H., 1998: Overview of the Po Valley fog experiment 1994 (CHEMDROP), Contr. Atmos. Phys. **71**, 3–19.

Gill P.S., Graedel T.E. and Weschler C.J., 1983: Organic films on atmospheric aerosol particles, fog droplets, cloud droplets, raindrops and snowflakes. Rev. Geophys. Space Phys. **21** 903–920.

Hänel G., 1976: The properties of atmospheric aerosol particles as functions of the relative humidity at thermodynamic equilibrium with the surrounding moist air. In: Landsberg, H.E. and Miegem, J. (eds.), Adv. Geophys., Academic Press, New York, 73–188

Hänel G., 1987: The role of aerosol properties during condensational stage of cloud: a reinvestigation of numerics and microphysics. Contr. Atmos. Phys. **60**, 321–339

Heintzenberg J., Wendisch M., Yuskiewicz B., Orsini D., Wiedensohler A., Stratmann F., Frank G., Martinsson B.G., Schell D., Fuzzi S. and Orsi, G., 1998: Characteristics of haze, mist and fog. Contr. Atmos. Phys. **71**, 21–31.

Klett J.D., 1971: Ion transport to cloud droplets by diffusion and conduction, and the resulting droplet charge distribution. J. Atmos. Sci. **28**, 78–85.

Knollenberg R.G., 1981: Techniques for probing cloud microstructure. In: Hobbs, P.V. (ed), Clouds, their formation, optical properties and effects. Academic Press, New York, 15–91.

Laaksonen A., Korhonen P., Kulmala M. and Charlson R.J., 1997: Modification of the Köhler equation to include soluble trace gases and slightly soluble substances. J. Atmos. Sci., in press.

Laj P., Fuzzi S., Lazzari A., Ricci L., Orsi G., Berner A., Dusek U., Schell D., Günther G., Wendisch M., Wobrock W., Frank G., Martinsson B.G. and Hillamo R., 1998: The size dependend composition of fog drops. Contr. Atmos. Phys. **71**, 115–131.

Lemmel G. and Novakov T., 1995: Water nucleation properties of carbon black and diesel soot particles. Atmos. Environ. **29**, 813–823

Martinsson B.G., 1996: Physical basis for a droplet aerosol analysing method. J. Aerosol Sci. **27**, 997–1013.

Martinsson B.G., Cederfelt S.-I., Svenningsson B., Frank G., Hansson H.-C., Swietlicki E., Wiedensohler A., Wendisch M., Gallagher M.W., Colvile R.N., Beswick K.M., Choularton T.W. and Bower K.N., 1997: Experimental determination of the connection between cloud droplet size and its dry residue size: Atmos. Environ. **31**, 2477–2490.

Noone K.J., Charlson R.J., Covert D.S., Ogren J.A. and Heintzenberg J., 1988: Cloud droplets: Solute concentration is size dependent. J. Geophys. Res. **93**, 9477–9482.

Noone K.J., Ogren J.A., Hallberg A., Heintzenberg J., Ström J., Hansson H.-C., Svenningsson B., Wiedensohler A., Fuzzi S., Facchini M.C., Arends B.G. and Berner A., 1992: Changes in aerosol size- and phase distributions due to physical processes in fog. Tellus **44B**, 489–504

Ogren J.A., Heintzenberg J., Zuber, A., Noone K.J. and Charlson R.J., 1989: Measurements of the size-dependence of solute concentration in cloud droplets. Tellus **41B**, 24–31.

Ogren J.A. and Charlson R.J., 1992: Implications for models and measurements of chemical inhomogenities among cloud droplets. Tellus **44B**, 208–225.

Ogren J.A., Noone K.J., Hallberg A., Heintzenberg J., Schell D., Berner A., Solly I., Kruisz C., Reischl G., Arends B.G. and Wobrock W., 1992: Measurements of the size dependence of concentration of non-volatile material in fog droplets. Tellus **44B**, 570–580.

Pandis S.N., Seinfeld J.H. and Pilinis C., 1990: The smog-fog-smog cycle and acid deposition. J. Geophys. Res. **95**, 18489–18500.

Pruppacher H.R. and Klett J.D., 1980: Microphysics of clouds and precipitation. D. Reidel, Dordrecht.

Pruppacher H.R. and Klett J.D., 1997: Microphysics of clouds and precipitation, 2nd ed. Kluwer, Dordrecht.

Ricci L., Fuzzi S., Laj P., Lazzari A., Orsi G., Berner A., Günther A., Jaeschke W., Wendisch M. and Arends B.G., 1998: Gas-Liquid Equilibria in Polluted Fog. Contr. Atmos. Phys. **71**, 159–170.

Saxena P., Hildemann L.M., McMurry P.H. and Seinfeld J.H., 1995: Organics alter hygroscopic behaviour of atmospheric particles. J. Geophys. Res. **100**, 18755–18770.

Shulman M.L., Jacobson M.C., Charlson R.J., Synovec R.E. and Young T.E., 1996: Dissolution behaviour and surface tension effects of organic compounds in nucleating cloud droplets. Geophys. Res. Lett. **23**, 277–280.

Svenningsson B., Hansson H.-C., Wiedensohler A., Noone K.J., Ogren J.A., Hallberg A. and Colvile R.N., 1994: Hygroscopic growth of aerosol particles and its influence on nucleation scavenging in cloud: Experimental results from Kleiner Feldberg. J. Atmos. Chem. **19**, 129–152.

Svenningsson B., Hansson H.-C., Martinsson B.G., Wiedensohler A., Swietlicki E., Cederfelt S.-I., Wendisch M., Bower K.N., Choularton T.W. and Colvile R.N., 1997: Cloud droplet nucleation scavenging in relation to the size and hygroscopic behaviour of aerosol particles. Atmos. Environ. **31**, 2463–2475.

Twohy C.H., Austin P.H. and Charlson R.J., 1989: Chemical consequences of the initial diffusional growth of cloud droplets: A clean marine case. Tellus **41B**, 51–60.

Wendisch M., Mertes S., Heintzenberg J., Wiedensohler A., Schell D., Wobrock W., Frank G., Martinsson B.G., Fuzzi S., Orsi G., Kos G. and Berner A., 1998: Drop size distribution and LWC in Po Valley fog. Contr. Atmos. Phys. **71**, 87–100.

Wobrock W., Jaeschke W., Schell D., Teichmann U., Wendisch M., Mertes S., Laubach J., Fuzzi S. and Orsi G., 1998: Observations of the turbulence structure of wind, temperature and liquid water content in a foggy surface layer. Contr. Atmos. Phys. **71**, 171–187.

Young K.C., 1993: Microphysical processes in clouds. Oxford University Press, New York, USA.

Yuskiewicz B., Orsini D., Stratmann F., Wendisch M., Wiedensohler A., Heintzenberg J., Martinsson B.G., Frank G., Wobrock W. and Schell D., 1998: Changes in submicrometer particle distributions and light scattering during haze and fog events in a highly polluted environment. Contr. Atmos. Phys. **71**, 33–45.